



OPEN ACCESS

EDITED BY

Paban Kumar Dash,
Defence Research & Development
Establishment (DRDE), India

REVIEWED BY

Lynette Isabella Oyier,
KEMRI Wellcome Trust Research
Programme, Kenya
Natarajan Gopalan,
Central University of Tamil Nadu, India

*CORRESPONDENCE

Karen P. Day

✉ karen.day@unimelb.edu.au

Shazia Ruybal-Pesántez

✉ s.ruybal@imperial.ac.uk

†PRESENT ADDRESS

Shazia Ruybal-Pesántez,
Department of Infectious Disease
Epidemiology and MRC Centre for Global
Infectious Disease Analysis, School of
Public Health, Imperial College London,
United Kingdom
Population Health and Immunity Division,
Walter and Eliza Hall Institute of Medical
Research, Melbourne, Australia
Instituto de Microbiología, Universidad San
Francisco de Quito, Ecuador
Claudia A. Vera-Arias,
Eck Institute for Global Health, University
of Notre Dame, Notre Dame, IN,
United States

SPECIALTY SECTION

This article was submitted to
Major Tropical Diseases,
a section of the journal
Frontiers in Tropical Diseases

RECEIVED 31 October 2022

ACCEPTED 02 March 2023

PUBLISHED 17 March 2023

CITATION

Ruybal-Pesántez S, Sáenz FE, Deed SL,
Johnson EK, Larremore DB, Vera-Arias CA,
Tiedje KE and Day KP (2023) Molecular
epidemiology of continued *Plasmodium*
falciparum disease transmission after an
outbreak in Ecuador.
Front. Trop. Dis 4:1085862.
doi: 10.3389/fitd.2023.1085862

Molecular epidemiology of continued *Plasmodium falciparum* disease transmission after an outbreak in Ecuador

Shazia Ruybal-Pesántez^{1*†}, Fabián E. Sáenz²,
Samantha L. Deed^{1,3}, Erik K. Johnson⁴, Daniel B. Larremore^{5,6},
Claudia A. Vera-Arias^{2†}, Kathryn E. Tiedje^{1,3} and Karen P. Day^{1,3*}

¹School of BioSciences/Bio21 Institute, The University of Melbourne, Melbourne, VIC, Australia, ²Centro de Investigación para la Salud en América Latina, Facultad de Ciencias Exactas y Naturales, Pontificia Universidad Católica del Ecuador, Quito, Ecuador, ³Department of Microbiology and Immunology, The University of Melbourne, Bio21 Institute and Peter Doherty Institute, Melbourne, VIC, Australia, ⁴Department of Applied Mathematics, University of Colorado Boulder, Boulder, CO, United States, ⁵Department of Computer Science, University of Colorado Boulder, Boulder, CO, United States, ⁶BioFrontiers Institute, University of Colorado Boulder, Boulder, CO, United States

To better understand the factors underlying the continued incidence of clinical episodes of falciparum malaria in E-2025 countries targeting elimination, we characterized the molecular epidemiology of *Plasmodium falciparum* disease transmission after a clonal outbreak in Ecuador. Here we study disease transmission by documenting the diversity and population structure of the major variant surface antigen of the blood stages of *P. falciparum* encoded by the *var* multigene family. We used a high-resolution genotyping method, “*var*coding”, involving targeted amplicon sequencing to fingerprint the DBL α encoding region of *var* genes to describe both antigenic *var* diversity and *var* repertoire similarity or relatedness in parasite isolates from clinical cases. We identified nine genetic *var*codes in 58 *P. falciparum* isolates causing clinical disease in 2013–2015. Network analyses revealed that four of the *var*codes were highly related to the outbreak *var*code, with identification of possible diversification of the outbreak parasites by recombination as seen in three of those *var*codes. The majority of clinical cases in Ecuador were associated with parasites with highly related or recombinant *var*codes to the outbreak clone and due to local transmission rather than recent importation of parasites from other endemic countries. Sharing of types in Ecuadorian *var*codes to those sampled in South American *var*codes reflects historical parasite importation of some *var*codes, especially from Colombia and Peru. Our findings highlight the translational application of *var*coding for outbreak surveillance in epidemic/unstable malaria transmission, such as in E-2025 countries, and point to the need for surveillance of local reservoirs of infection in Ecuador to achieve the malaria elimination goal by 2025.

KEYWORDS

malaria elimination, antigenic diversity, disease transmission, outbreak, genomic epidemiology, molecular surveillance, *var* DBL α , *Plasmodium falciparum*

Introduction

A recent global push for national malaria elimination in 21 countries by 2020 led to three being declared malaria-free (Algeria, El Salvador and Paraguay), but the target was not met for the remaining countries (1, 2). These countries are now part of a renewed initiative launched by the WHO in 2021 supporting a total of 25 countries, known as E-2025 countries, with the shared goal to eliminate local transmission of malaria by 2025 by reducing the incidence of indigenous or locally transmitted cases to zero (2). These countries include Mexico, Panama, Ecuador, South Africa, Eswatini, Thailand, Malaysia, among others. Malaria transmission in many of these countries is epidemic/unstable with risks of outbreaks, parasite importation, and resurgent malaria (3–5).

Ecuador, one of the nine E-2025 countries in Latin America, did not meet the 2020 elimination target due to malaria resurgence since 2015 (2, 6, 7). Malaria elimination efforts in Ecuador have largely focused on tropical areas, specifically the northwest coast and the Amazon region (8–12). These areas border non E-2025 countries, Colombia and Peru, that still have endemic and moderate to low transmission (13–20). Clinical cases caused by *P. falciparum* are mostly concentrated in the northwest coast and Ecuador has epidemic/unstable *P. falciparum* transmission, with *P. vivax* being the dominant species. Determining whether the continued incidence of *P. falciparum* clinical cases is due to imported or locally acquired parasites is of key public health interest to better understand disease transmission patterns and aid decision-making to allocate limited resources to achieve the E-2025 elimination goal.

Application of genotyping methods to epidemiological analyses can aid public health responses in such settings by informing on parasite diversity and relatedness to identify imported cases and characterize residual and/or resurgent disease transmission patterns with higher resolution than routine case incidence monitoring (21, 22). Such epidemiological surveys can be impactful in delineating malaria transmission hotspots, if any, within an endemic area. Molecular surveillance to characterize malaria transmission patterns has relied on genotyping neutral molecular markers such as microsatellites or single-nucleotide polymorphisms (SNPs) as more cost-effective approaches than whole genome sequencing. Of relevance to low or epidemic transmission, neutral variation has been commonly used to inform about clonality and relatedness as well as track genomes spatially. Genes under selection can provide an alternative but complementary view of microevolution (23–25).

Molecular surveillance based on diversity of the genes encoding the major surface antigen of pathogens is a well-established microbiological paradigm typically used in virology (e.g. Influenza A, HIV-1, SARS-CoV-2) and bacteriology (e.g. *Neisseria* spp, *Streptococcus pyogenes*) because genotyping such antigens provides important information on recombination rates, the factors associated with these recombination events, and transmission dynamics. Employing this surveillance approach is however more complex in *falciparum* malaria where the major variant surface antigen of the blood stages known as PfEMP1 is encoded by the *var* multigene family with 40–60 *var* genes per genome (26) and extensive diversity of *var* genes exists in parasite

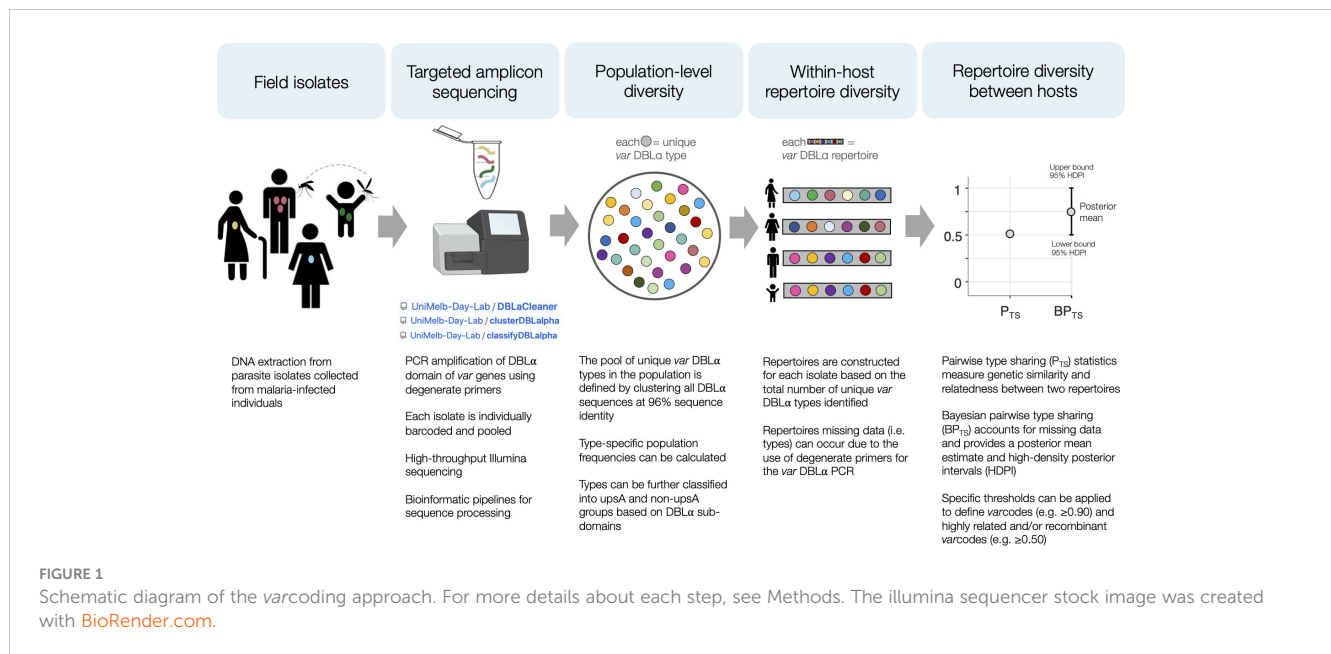
populations (27). Indeed, *var* diversity has been shown to be correlated with transmission intensity with the highest diversity, in the order of tens of thousands of variants, seen in African populations and the lowest in the Americas, in the order of hundreds (27–31). *Var* genes and repertoires diversify by meiotic recombination during the obligatory sexual phase of the life cycle in the mosquito as well as by mitotic recombination. We define a fingerprint of the *var* repertoire of an isolate by genotyping the highly diverse DBL α tag of the *P. falciparum* *var* multigene family (29–33). This fingerprinting method we call “*var*coding” requires a single PCR with degenerate primers followed by amplicon deep sequencing. We sample DBL α diversity of *P. falciparum* within and between human hosts, as well as measure similarity or relatedness between *var* repertoires we call *var*codes. Bayesian statistics are used to account for variable sampling of all members of the multigene family (genomes contain 40–60 *var* genes) in field samples when amplifying low-quality parasite DNA with degenerate primers and to quantify the uncertainty around relatedness estimates (Figure 1). This analytical approach was designed specifically for *var* genes under immune selection where alleles per se cannot be assigned since chromosomal positions are unknown, and commonly used approaches to infer relatedness such as identity-by-descent (IBD) are not straightforward to apply due to the complexities of this multi-copy *var* gene family.

Here, we apply *var*coding for the first time in unstable, epidemic malaria to look at diversity and population structure of these immune evasion genes. Specifically, we characterize the transmission of clinical *P. falciparum* cases in Ecuador during and up to two years after an outbreak in 2012–2013, which was previously found to be clonal by microsatellite genotyping (i.e., caused by a single parasite lineage) (19). Analysis of *var*code relatedness networks allowed us to define different genomic parasite lineages (or *var*codes) circulating locally, as well as detect signatures of highly related parasites and possibly recently recombined genomes with respect to *var* repertoires. Parasites with the *var*code of the outbreak clone or recombinant/highly related *var*codes relative to the outbreak clonal lineage were predominantly associated with the continued incidence of clinical cases after the outbreak. Hot spots for *var*code diversity were identified suggestive of the existence of local reservoirs of infection. Further comparative analyses to published data from historical South American isolates (30) elucidated possible origins of Ecuadorian parasites, demonstrating that the majority of clinical cases were due to local transmission and not recent importation.

Methods

Study design and sample collection

In this molecular epidemiological study, we examined *P. falciparum* isolates collected from 2013–2015 in Ecuador from individuals of all ages presenting with uncomplicated malaria cases confirmed by microscopy and/or PET-PCR (34). Details on the study population and data collection have been previously



published (19, 35, 36). Briefly, these samples were collected during passive surveillance by the Ecuadorian Ministry of Health from consenting participants who lived in the areas where the samples were taken, were over 2 years old, agreed to participate and provided a blood sample (either venous blood or dried blood spot) and answered a basic demographic questionnaire (including places recently travelled and their address). Genomic DNA was extracted from venous blood or dried blood spots using a QIAamp DNA MINI KIT (QIAGEN, USA) as recommended by the manufacturer. The study was approved by the ethics committees at the Pontificia Universidad Católica del Ecuador (Quito, Ecuador) and The University of Melbourne (Melbourne, Australia).

Var DBL α amplification and sequencing

Var genotyping PCR, sequencing details, and related data processing steps have been previously published (33, 37). Briefly, for each *P. falciparum* isolate, a single-step PCR to amplify the DBL α domains of var genes was performed using universal degenerate primers targeting homology blocks D (forward primer) and H (reverse primer) originally described in (38), with the addition of 10bp GS FLX Titanium multiplex identifier primer sequence for barcoding (39). The PCR reaction was prepared in a total volume of 40 μ l, containing 3 μ l of genomic DNA, MgCl $_2$ at a final concentration of 2mM, dNTPs at a final concentration of 0.07mM, each primer at a final concentration of 0.375mM and 3 units of Flexi DNA Taq polymerase (Promega). The cycling conditions were as follows: initial denaturation step of 2 min at 95°C was followed by 30 cycles of: annealing for 40 seconds at 95°C, extension for 90 seconds at 49°C, denaturation for 90 seconds at 65°C, and then a final extension step of 10 min at 65°C. The resulting individually barcoded DBL α amplicons (approximately 450-700bp in length) were pooled equimolarly and barcoded libraries were prepared using the KAPA Low-Throughput Library Preparation Kit

(Kapa Biosystems). The libraries were sequenced on a MiSeq Illumina platform using the 2x300bp paired-end protocol and MiSeq Reagent kit v3 chemistry (Australian Genome Research Facility, Melbourne, Australia).

Var DBL α data processing

The raw illumina sequence data was then cleaned and processed using the DBL α Cleaner pipeline [(37, 40), <http://github.com/Unimelb-Day-Lab/DBLalphaCleaner>]. Our customized bioinformatic pipeline has been described in detail in (37, 40). Briefly, we demultiplexed and merged the paired reads as well as removed low-quality reads and chimeras using several filtering parameters (see Supplementary Figure S1 for details). This pipeline resulted in 2,141 cleaned DBL α sequences (Supplementary Figure S1). To identify distinct or unique DBL α types (i.e., unique genetic variants), we clustered the DBL α sequences from Ecuadorian *P. falciparum* isolates with 5,699 previously published (30) DBL α sequences from other South American countries (Colombia (N=21 isolates), French Guiana (N=76 isolates), Peru (N=21 isolates), and Venezuela (N=10 isolates) at the standard 96% sequence identity (32) using the clusterDBLalpha pipeline (<http://github.com/Unimelb-Day-Lab/clusterDBLalpha>). We further curated our dataset by translating the DBL α types into amino acid sequences using the classifyDBLalpha pipeline (<http://github.com/Unimelb-Day-Lab/classifyDBLalpha>) and removing any DBL α types that were non-translatable (N=4). All the cleaned DBL α sequences in this study (Supplementary Figure S1) have been submitted to the DDBJ/ENA/GenBank (BioProject Number: PRJNA642683). A tutorial on the DBL α processing pipelines can be found at <http://github.com/Unimelb-Day-Lab/tutorialDBLalpha>.

In addition, any *P. falciparum* isolate with low sequencing quality (< 10 DBL α types) was removed from the analysis. Therefore, from a total of 70 genotyped *P. falciparum* Ecuadorian

isolates, 12 *P. falciparum* isolates with low DNA quality and/or poor sequencing quality were removed and we obtained *var* DBL α data for 58 isolates (82.9%). A total of 543 unique DBL α types identified in the 186 South American *P. falciparum* isolates [N = 58 Ecuadorian *P. falciparum* isolates from this study, N = 128 South American *P. falciparum* isolates previously published in (30)] were used for subsequent *var* analyses at the regional-level, and only the 195 unique DBL α types identified in Ecuador were used for Ecuador-specific analyses. To evaluate how well we sampled the true pool of *var* DBL α diversity (i.e., the true number of genetic variants circulating) in Ecuador and in South America, we used the R package *vegan* (41) to generate species accumulation curves where the number of unique DBL α types are plotted as a function of the number of sampled sequences. Plateauing of this curve indicates saturation and robust sampling of the diversity pool (i.e. sampling more sequences will not identify any new types).

Genetic relatedness analyses

Measuring pairwise type sharing

To estimate *varcode* similarity or relatedness between all isolate pairs, we calculated the similarity index Pairwise Type Sharing (P_{TS}) (28), as adapted by He et al. (37) to account for differences in DBL α sampling across isolates (i.e. differences in isolate repertoire sizes), and unbiased Bayesian pairwise type sharing estimates (BP_{TS}) to further account for uncertainty in P_{TS} estimates. P_{TS} represents the proportion of shared DBL α types between an isolate pair. It is calculated directionally by dividing the number of shared DBL α types, N_s , between two isolates *a* and *b*, by the total number of DBL α types in each isolate or repertoire size, N_a or N_b . Thus, for each pair of isolates we calculate $P_{TS(a,b)} = N_s/N_a$ and $P_{TS(b,a)} = N_s/N_b$.

Varcode relatedness can also be explored more rigorously with unbiased Bayesian pairwise type sharing (BP_{TS}) (42, 43). This approach uses Bayesian inference methods, which estimate repertoire overlap and uncertainty, and uses them in a subsequent P_{TS} calculation, carrying that uncertainty forward. The prior distribution for repertoire size, used in inference, was informed by observations as follows. First, the median observed repertoire size in Ecuadorian isolates was 37 types, ranging from 11 to 43 (Supplementary Table S1). Second, the number of expected *var* genes with DBL α domains from whole genome sequencing data of the Honduran laboratory reference strain HB3 was 42 (26) and 50 *var* genes based on long-read PacBio sequencing of HB3 (44). And third, based on our sequencing data of 37 technical replicates of HB3, the median repertoire size or number of DBL α types per isolate was 39 (range 36-41 types), with 40 types consistently identified in the majority of replicates (range 21-37 replicates). We therefore used a uniform prior on repertoire sizes between 40 and 50 types, combined with the general Bayesian repertoire overlap framework (42) to produce unbiased estimates (posterior means). These were used to confirm our P_{TS} estimates. As expected, the P_{TS} and BP_{TS} estimates were positively correlated (Pearson's correlation coefficient = 0.919, $p < 0.001$, Supplementary Figure S3). To measure uncertainty in central estimates, we computed a 95%

highest density posterior interval (HDPI), a Bayesian version of confidence intervals, for each pairwise estimate. Like a frequentist confidence interval, the width of the HDPI provides a measure of uncertainty of each pairwise comparison. All posteriors were sampled using Markov chain Monte Carlo.

Interpretation of *varcode* relatedness measures

Every parasite isolate was compared to every other parasite isolate in the population to determine the proportion of shared DBL α types. Theoretically, pairwise comparisons resulting in P_{TS} of 0 (0% shared types), 0.5 (50% shared types), and 1 (100% shared types) will reflect genetically distinct isolates with different *var* repertoires, isolates with recombinant or highly related *var* repertoires, and clones or genetically identical isolates with the same *var* repertoire, respectively. In practice, however, in low-transmission areas often “fixed” relatedness thresholds may obscure true relatedness estimates because of inbreeding events and thus require confirmation by measuring the uncertainty around each estimate with methods like our Bayesian inference of P_{TS} . We applied this approach to define “*varcodes*” as groups of isolates sharing $\geq 90\%$ of their DBL α types ($P_{TS} \geq 0.90$), identifying putatively identical genomes within the margin of error of detection of 1-5 DBL α types in an isolate. We confirmed our interpretations of *varcodes*, recombinants/highly related, and genetically distinct isolates at the thresholds of 0, 0.5 and 0.90-1, respectively, by comparing to unbiased BP_{TS} estimates (posterior means) and examining the HDPI.

Visualization of *varcode* relatedness networks

To visualize the *varcode* relatedness between isolates as determined by P_{TS} or BP_{TS} , we constructed networks using the R packages *ggraph* (45) and *tidygraph* (46) where isolates are depicted as nodes and edges as the P_{TS} or BP_{TS} values at a given threshold. The R package *ggsatial* (47) was used to plot spatial networks using latitude/longitude coordinates for sampling location. To visualize *varcode* relatedness of parasites over time we used the R package *gganimate* (48) to construct spatiotemporal relatedness networks. We generated a clustered heatmap based on the presence/absence matrix of DBL α types to visualize the genetic profiles of each isolate in Ecuador and each country in South America using the R package *heatmap* (49) and the “complete” clustering method. Unrooted neighbor-joining phylogenetic trees based on pairwise genetic distance (calculated as $1 - P_{TS}$) were constructed using the R packages *ape* (50) and *ggtree* (51, 52).

Statistical analysis

We used R version 3.5.2 (53), base R, and the R packages *dplyr* (54), *epiR* (55) for all analyses. We used chi-squared tests for

univariate analyses of categorical variables to compare proportions and for non-parametric tests to compare distributions of continuous variables between two groups (Mann-Whitney U test) or among k groups (Kruskal-Wallis test), with a Bonferroni correction for multiple comparisons.

Results

Limited var diversity in Ecuadorian *P. falciparum* populations

Diversity of *var* genes was assessed by *var*coding for 58 *P. falciparum* isolates that were collected between 2013 and 2015 from individuals of all ages experiencing clinical malaria (Figure 2). These isolates represent 21% of the total cases reported in 2013, 61% in 2014, and 3% in 2015 (60% of the cases reported in January, 7% in May and 8% in November 2015). Overall, we identified 195 unique DBL α variants or types from 2,141 DBL α sequences (Supplementary Figure S1) from the 58 isolates, representative of the diversity circulating in Ecuadorian *P. falciparum* populations, as indicated by sampling accumulation curves approaching a plateau (Supplementary Figure S2).

Defining nine distinct *var*codes circulating in Ecuador and describing spatiotemporal disease transmission trends

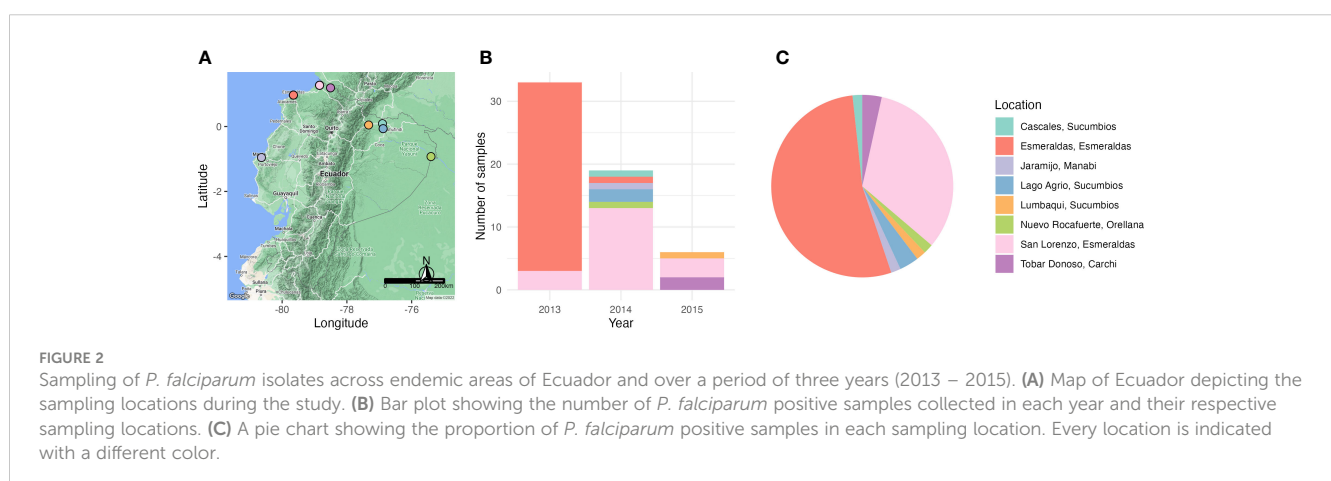
To define distinct *var*codes circulating locally in Ecuador, we estimated relatedness between two isolates' *var*codes by calculating the similarity index, Pairwise Type Sharing (P_{TS}) and constructed relatedness networks to identify genomes with the same *var*codes ($P_{TS} \geq 0.90$). We confirmed this by comparing *var*codes derived from P_{TS} to those derived from posterior mean BP_{TS} estimates (Supplementary Figure S3), which include statistical uncertainty, and by examining the lower and upper bounds of the 95% highest density posterior intervals (HDPIs). This revealed nine genetically distinct *var*codes in this study with 36 isolates having *var*code1 (representing the clonal outbreak in Esmeraldas City, salmon pink

*var*code Figures 3 and Figure 4A) and at the other extreme *var*code4, *var*code5, *var*code9 were seen only once (Figure 4A, S4A). Our definition of *var*codes proved to predict genomic lineages (identity-by-descent ≥ 0.99) based on published whole genome sequence data in the case of 30 of the isolates (six *var*codes) that were analyzed by both WGS (56) and *var*coding. As expected, the outbreak *var*code1 was clonal (indicated by HDPIs that included 1; Figure S5B), as previously demonstrated by microsatellite genotyping (19) and more recently by WGS (56). The outbreak *var*code1 identified in Esmeraldas City was also identified in San Lorenzo, Esmeraldas (~150km from Esmeraldas City) in 2013, then Cascales, Sucumbios (>300km away) in 2014, and then in Tobar Donoso, Carchi (~150km away) in 2015 (Figure 4B). Overall, persistent disease transmission of the same *var*codes was observed both over time (Figure 4B) and large distances (Figures 3A–C). The median time between first and last identification of the same *var*codes with any clinical case was 216 days or approximately 7 months (range = 190 – 823 days) during the study period. This is in line with reports in Peru (57) and Colombia (18, 58) where clonal parasites were shown to be circulating up to five and eight years after first identification, respectively.

*Var*code relatedness networks reveal signatures of highly related parasites and local disease transmission

We next constructed spatiotemporal *var*code relatedness networks to explore signatures of local disease transmission after the outbreak. Figure 4C shows that 15 isolates with four *var*codes (*var*code3, *var*code4, *var*code6, *var*code7) clustered with the outbreak *var*code1 at the threshold of $P_{TS} \geq 0.50$ (Figure 4C). The remaining 7 isolates with different *var*codes did not cluster in the network and were genetically distinct. These patterns were confirmed using BP_{TS} estimates based on posterior means (Supplementary Figure S6A) and their corresponding 95% HDPIs (Supplementary Figures S5C–F, S6B, C).

To better understand the *var*code relatedness signatures in the “outbreak cluster” we examined both P_{TS} and BP_{TS} estimates. In some instances, highly related *var*codes shared ~50% of the outbreak DBL α types, such as the outbreak *var*code1 with



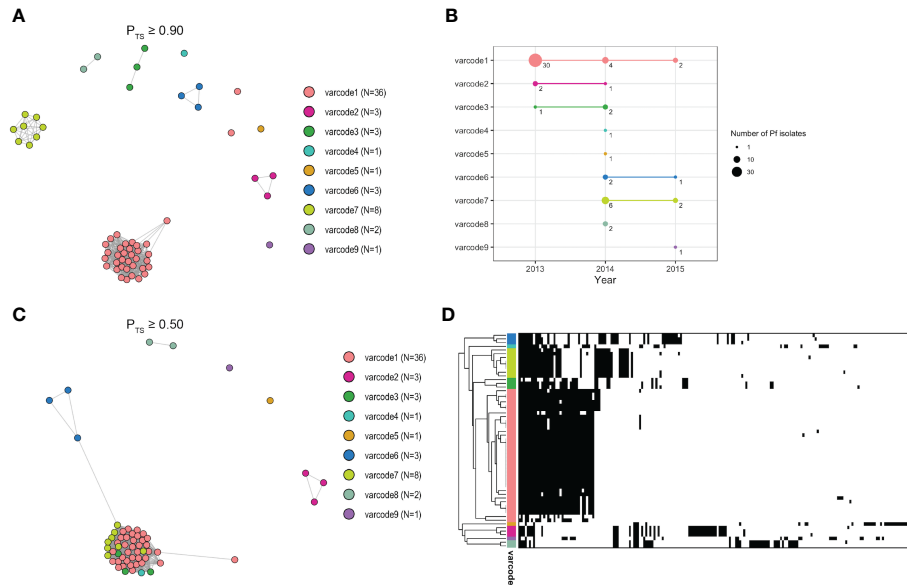


FIGURE 3
Varcode relatedness networks in Ecuador (A) A network visualization of the varcode relatedness of *P. falciparum* isolates at the threshold of $P_{TS} \geq 0.90$ to define varcodes (see Methods). Every node represents a *P. falciparum* isolate and an edge represents the P_{TS} value between two particular nodes/isolates. Isolates that cluster together (i.e., connected by edges) are considered to have the same varcode. Each color represents a different varcode. Two *P. falciparum* isolates belonging to outbreak varcode1 appear as outliers in the network due to undersampling of their DBL α types. N refers to the number of isolates. For comparison to BP_{TS} estimates see [Supplementary Figures S4, S5](#). **(B)** The number of *P. falciparum* isolates within each varcode (i.e., size of circle) in each year and their persistence over time. The three varcodes (varcode1, varcode2, varcode3) identified in 2013 were identified again in 2014, and outbreak varcode1 was identified again in 2015. Two varcodes identified in 2014 (varcode6, varcode7) were also identified in 2015. **(C)** A network visualization of the genetic relatedness of varcodes at the threshold of $P_{TS} \geq 0.50$ to discriminate between highly related/recombinant varcodes and genetically distinct varcodes. Isolates/varcodes that cluster together (i.e., connected by edges) represent highly related/recombinants. For comparison to BP_{TS} estimates see [Supplementary Figures S5, S6](#). **(D)** A clustered heatmap showing the genetic profiles of each *P. falciparum* isolate with rows representing each isolate and columns representing each DBL α type. Black and white denote the presence and absence of each type, respectively. Isolates that clustered together were more genetically similar (i.e., the same DBL α types were present). Similarly, varcodes that clustered together were more genetically similar (e.g., highly related/recombinants).

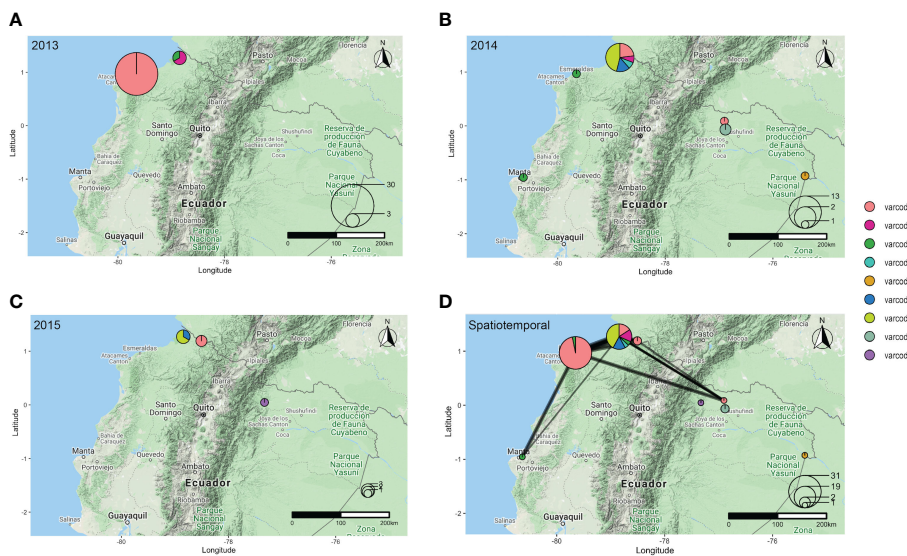


FIGURE 4
 The spatial distribution of varcodes in **(A)** 2013, **(B)** 2014, **(C)** 2015, with the size of the circle representing the number of *P. falciparum* isolates sampled in a given location in each year and the pie chart depicting the proportion of each varcode identified. **(D)** Spatiotemporal varcode relatedness network between 2013–2015. Every node represents a sampling location, the size of the circle represents the number of *P. falciparum* isolates sampled in each location, the pie chart depicts the proportion of each varcode identified, and the weighted edges show genetically related varcodes ($P_{TS} \geq 0.50$).

*varcodes*3,4,6,7 (median P_{TS} range=37-58%, median BP_{TS} =45-70%, **Figures S5C, D**). This level of *varcode* relatedness would be consistent with the generation of a new *varcode* through outcrossing by conventional meiosis resulting in recombinant *var* repertoires of the outbreak clone. When examining the pairwise combinations of *varcodes* 3,4,6,7, sharing of types also indicates high relatedness (median P_{TS} range=27-50%, median BP_{TS} =32-64%, **Figures S5C, D**), pointing to the possibility of a prior cross followed by a backcross given the overall limited *var* diversity in the parasite population. However, the timing of such crosses is unknown. Interestingly, all the possibly recombinant and highly related *varcodes* (*varcodes*3,4,6,7) were identified in San Lorenzo with *varcode*7 being the main one, indicating this area is a transmission hot spot and a reservoir of parasites with diverse *var* repertoires (**Figure 3D**).

To further confirm the observed *varcode* relatedness signatures, we constructed a clustered heatmap to visualize the genetic profiles of each isolate based on the presence/absence of the 195 DBL α types, such that genetically similar isolates cluster together (**Figure 4D**). This analysis confirmed that in the case of isolates identified as highly related to the outbreak *varcode*1, a proportion of outbreak DBL α types as well as different DBL α types were present. By contrast, the genetic profiles of isolates with *varcodes* 2, 5, 8, and 9 had more different DBL α types to all other *varcodes*, i.e., parasites with genetically distinct *varcodes*, with sharing of only <30% of types in most instances (median P_{TS} range= 2-29% except for 2 pairwise comparisons 34-37%; median BP_{TS} range=4-30% except for 5 pairwise comparisons 31-41%, **Figures S5E, F**).

Parasites with highly related/recombinant *varcodes* were most frequently associated with *P. falciparum* clinical episodes following the 2012-13 outbreak

Prior to the outbreak there had been a steady decline in clinical cases; however, increased incidence of disease occurred after the outbreak. Therefore, we analyzed trends in the epidemiology of *P. falciparum* cases that occurred post-outbreak to understand if there were any key risk factors. Of the 25 individuals in our study that had a clinical *P. falciparum* episode post-outbreak, we had age data for 18 individuals (72%, **Table 1**). There was no significant difference (Kruskal-Wallis test, $p = 0.65$) in the median age of individuals experiencing clinical episodes caused by parasites with the outbreak *varcode*1 (19 years, range = 19 – 57 years, $N = 3$ patients), a highly-related/recombinant of *varcode*1 (i.e., *varcodes* 3, 4, 6, or 7) (25 years, range = 17 – 58 years, $N = 13$ patients), or by a different *varcode* (34.5 years, range = 32 – 37 years, $N = 2$ patients). A greater diversity of *varcodes* (1-9 inclusive) was associated with incidence of clinical malaria post-outbreak than during the 2013 outbreak (*varcodes* 1,2,3). Indeed in 2014, 79% of the cases sampled were caused by either parasites with the outbreak *varcode*1 (21%) or with any of the four highly-related/recombinants of *varcode*1 (58%). The trend was similar in 2015 with 83% of the cases sampled caused by either parasites with the outbreak *varcode*1 (33%) or with any of the four highly-related/recombinants of *varcode*1 (50%), although our

sampling of reported cases in 2015 after January was limited. Importantly, overall, we found that 80% of the cases sampled after the outbreak were caused by either parasites with the outbreak *varcode*1 (24%) or with any of the four highly-related/recombinants of *varcode*1 (56%), especially with *varcode*7 (representing 57% of the cases caused by parasites with highly-related/recombinant *varcodes*). Thus, disease transmission after the outbreak in 2014 and into 2015 was predominantly associated with parasites with highly related/recombinant *var* repertoires of the outbreak clone, with most of these cases occurring in the San Lorenzo hotspot.

Comparative analyses to South America: elucidating possible origins of Ecuadorian *varcodes* and signatures of historical importation

We next examined the possible origins of the *varcodes* circulating locally in Ecuador by comparing to the only published *var* DBL α dataset from the region (30), comprising 128 *P. falciparum* isolates collected from South American *P. falciparum* populations in 2002-2008 from countries with higher malaria transmission compared to Ecuador (**Figure 5A**). In all countries (except some isolates in French Guiana), the number of DBL α types per isolate repertoire, a proxy for complexity of infection (COI, i.e. the number of *P. falciparum* genomes in an infection), was indicative of only one *P. falciparum* genome infecting an individual (i.e., repertoire size ≤ 50 or COI=1, **Supplementary Figure S9; Supplementary Table S1**). Despite the difference in sampling years, the 543 unique DBL α types identified in these 186 isolates represent the diversity circulating in South American *P. falciparum* populations, as indicated by DBL α sampling accumulation curves approaching saturation (**Supplementary Figure S7**). An unrooted phylogenetic neighbor-joining tree showing pairwise genetic distance ($1-P_{TS}$) revealed distinct, country-specific clusters of isolates with related *varcodes* (**Figure 5B**), consistent with previous analyses demonstrating geographic population structure (30). Thus, despite the relatively low *var* diversity, there is sufficient resolution to differentiate between the parasite populations from different South American countries and to explore the possible geographic origins at the level of country-specific DBL α types but also the unique combinations of these types as *varcodes*.

Varcoding resolved a total of 97 *varcodes* in South America ($P_{TS} \geq 0.90$), ranging from nine in Ecuador and Venezuela, to 56 *varcodes* in French Guiana and the *varcodes* were country-specific since none of the isolates from different countries clustered with isolates from another country at this threshold (**Supplementary Figure S8**). However, although identical *varcodes* were not identified in multiple countries, we were interested in examining *varcode* relatedness. To assess the overall sharing of types in the *varcodes* identified in Ecuador to those sampled in other South American parasite populations, we aggregated all possible DBL α types identified in the isolates comprising each Ecuadorian *varcode* (range: 34-47 types per *varcode*) and all DBL α types seen in any isolate from a

TABLE 1 Epidemiological characteristics of study participants.

Case	Month collected		Age range, years	Sex	Sampling location (County, Province)	Self-reported infection location*	varcode	Putative origin**
EC1	Jan 2013	<i>Outbreak</i>	NA	NA	Esmeraldas City, Esmeraldas		varcode1	Local
EC2	Jan 2013	<i>Outbreak</i>	NA	NA	Esmeraldas City, Esmeraldas		varcode1	Local
EC3	May 2013	<i>Outbreak</i>	>30-40	M	Esmeraldas City, Esmeraldas		varcode1	Local
EC4	May 2013	<i>Outbreak</i>	>30-40	M	Esmeraldas City, Esmeraldas		varcode1	Local
EC5	May 2013	<i>Outbreak</i>	>50-60	F	Esmeraldas City, Esmeraldas		varcode1	Local
EC6	May 2013	<i>Outbreak</i>	>30-40	M	Esmeraldas City, Esmeraldas		varcode1	Local
EC7	May 2013	<i>Outbreak</i>	>50-60	F	Esmeraldas City, Esmeraldas		varcode1	Local
EC8	May 2013	<i>Outbreak</i>	>10-20	F	Esmeraldas City, Esmeraldas		varcode1	Local
EC9	May 2013	<i>Outbreak</i>	>10-20	F	Esmeraldas City, Esmeraldas		varcode1	Local
EC10	May 2013	<i>Outbreak</i>	>10-20	M	Esmeraldas City, Esmeraldas		varcode1	Local
EC11	May 2013	<i>Outbreak</i>	>20-30	F	Esmeraldas City, Esmeraldas		varcode1	Local
EC12	Jun 2013	<i>Outbreak</i>	>10-20	F	Esmeraldas City, Esmeraldas		varcode1	Local
EC13	Jun 2013	<i>Outbreak</i>	>10-20	M	Esmeraldas City, Esmeraldas		varcode1	Local
EC14	Jun 2013	<i>Outbreak</i>	>40-50	M	Esmeraldas City, Esmeraldas		varcode1	Local
EC15	Jun 2013	<i>Outbreak</i>	>40-50	M	Esmeraldas City, Esmeraldas		varcode1	Local
EC16	Jun 2013	<i>Outbreak</i>	>10-20	F	Esmeraldas City, Esmeraldas		varcode1	Local
EC17	Jun 2013	<i>Outbreak</i>	>10-20	F	Esmeraldas City, Esmeraldas		varcode1	Local
EC18	Jun 2013	<i>Outbreak</i>	>20-30	M	Esmeraldas City, Esmeraldas		varcode1	Local
EC19	Jun 2013	<i>Outbreak</i>	>40-50	M	Esmeraldas City, Esmeraldas		varcode1	Local
EC20	Jul 2013		>20-30	M	San Lorenzo, Esmeraldas		varcode2	Local
EC21	Jul 2013		>10-20	F	San Lorenzo, Esmeraldas		varcode2	Local
EC22	Jul 2013	<i>Outbreak</i>	>10-20	M	Esmeraldas City, Esmeraldas		varcode1	Local
EC23	Jul 2013	<i>Outbreak</i>	>0-10	M	Esmeraldas City, Esmeraldas		varcode1	Local
EC24	Jul 2013	<i>Outbreak</i>	NA	F	Esmeraldas City, Esmeraldas		varcode1	Local
EC25	Sep 2013	<i>Outbreak</i>	>30-40	M	Esmeraldas City, Esmeraldas		varcode1	Local
EC26	Oct 2013	<i>Outbreak</i>	>20-30	F	Esmeraldas City, Esmeraldas		varcode1	Local
EC27	Oct 2013		>10-20	F	San Lorenzo, Esmeraldas		varcode3	Local
EC28	Oct 2013	<i>Outbreak</i>	>20-30	M	Esmeraldas City, Esmeraldas		varcode1	Local
EC29	Nov 2013	<i>Outbreak</i>	>10-20	M	Esmeraldas City, Esmeraldas		varcode1	Local
EC30	Nov 2013	<i>Outbreak</i>	>10-20	M	Esmeraldas City, Esmeraldas		varcode1	Local
EC31	Nov 2013	<i>Outbreak</i>	>10-20	F	Esmeraldas City, Esmeraldas		varcode1	Local
EC32	Nov 2013	<i>Outbreak</i>	>30-40	M	Esmeraldas City, Esmeraldas		varcode1	Local
EC33	Nov 2013	<i>Outbreak</i>	>30-40	M	Esmeraldas City, Esmeraldas		varcode1	Local
EC34	Jan 2014		NA	NA	Jaramijo, Manabi		varcode3	Local
EC35	Jan 2014		>50-60	F	San Lorenzo, Esmeraldas		varcode1	Local
EC36	Jan 2014		>10-20	M	San Lorenzo, Esmeraldas		varcode1	Local
EC37	Jan 2014		>30-40	M	San Lorenzo, Esmeraldas		varcode2	Local
EC38	Jan 2014		>10-20	M	San Lorenzo, Esmeraldas		varcode4	Local

(Continued)

TABLE 1 Continued

Case	Month collected		Age range, years	Sex	Sampling location (County, Province)	Self-reported infection location*	varcode	Putative origin**
EC39	Jan 2014		>10-20	M	San Lorenzo, Esmeraldas		varcode1	Local
EC40	Jan 2014		>30-40	F	Nuevo Rocafuerte, Orellana	Peru	varcode5	French Guiana/ Peru/ Venezuela
EC41	Mar 2014		>20-30	M	San Lorenzo, Esmeraldas		varcode6	Local
EC42	May 2014		>50-60	F	Esmeraldas City, Esmeraldas	Colombia	varcode3	Local
EC43	May 2014		NA	NA	Cascales, Sucumbios	San Lorenzo, Esmeraldas	varcode1	Local
EC44	Jul 2014		>30-40	F	San Lorenzo, Esmeraldas		varcode7	Local
EC45	Aug 2014		>20-30	F	San Lorenzo, Esmeraldas		varcode7	Local
EC46	Aug 2014		>20-30	M	San Lorenzo, Esmeraldas		varcode7	Local
EC47	Aug 2014		>50-60	M	San Lorenzo, Esmeraldas		varcode7	Local
EC48	Aug 2014		>20-30	M	San Lorenzo, Esmeraldas		varcode7	Local
EC49	Sep 2014		NA	F	Lago Agrio, Sucumbios	Colombia	varcode8	Local
EC50	Oct 2014		NA	NA	Lago Agrio, Sucumbios	Colombia	varcode8	Local
EC51	Oct 2014		>30-40	M	San Lorenzo, Esmeraldas	Colombia	varcode6	Local
EC52	Dec 2014		>20-30	M	San Lorenzo, Esmeraldas		varcode7	Local
EC53	Jan 2015		NA	NA	Lumbaqui, Sucumbios	Colombia	varcode9	Colombia
EC54	Jan 2015		>20-30	M	San Lorenzo, Esmeraldas		varcode7	Local
EC55	Jan 2015		>10-20	M	San Lorenzo, Esmeraldas		varcode7	Local
EC56	Nov 2015		>10-20	F	San Lorenzo, Esmeraldas		varcode6	Local
EC57	May 2015		NA	NA	Tobar Donoso, Carchi		varcode1	Local
EC58	May 2015		NA	NA	Tobar Donoso, Carchi		varcode1	Local

NA refers to no data collected for that particular epidemiological variable.

*The self-reported infection location was recorded at the time of sample collection based on the answers provided by the study participants.

**The putative origin as determined by varcoding.

given country (range: 112-249 types per country). The overall sharing of types was high, with the highest median sharing with Peru (53%, range: 26-72%) followed by Colombia (39%, range: 19-89%) and Venezuela (27%, range: 12-76%), and only 10% with French Guiana (range: 3-86%) except for varcode5 (86%) (Figure 5D).

Next we estimated P_{TS} between all possible isolate pairs to examine whether any of the Ecuadorian parasites had varcodes that were genetically related to these historical South American parasites ($P_{TS} \geq 0.50$) and constructed regional varcode relatedness networks (Figure 5C). We identified a genetically related Peruvian *P. falciparum* isolate that clustered with the “outbreak cluster”, but especially with outbreak varcode1 ($P_{TS} = 0.66-0.75$ with varcode1 isolates). This is consistent with previous analyses using microsatellites showing the outbreak source was possibly a residual parasite lineage circulating in Peru in 1999-2000 and in Ecuador in the early 1990s (13, 19). More recent whole genome sequence data also points to the outbreak varcode1 circulating in Colombia in the early 2000s (56). No other South American isolate clustered with the “outbreak cluster” based on our network analysis,

suggesting that there may be other locally circulating parasites in unidentified reservoirs in Ecuador, e.g. the parental varcodes of the possible recombinants. In the case of varcode3, the WGS study showed that isolates with varcode1 and varcode3 belong to distinct genomic lineages but are identical by descent across 80% of the genome thus belong to a “super-cluster” (56), which is consistent with our BP_{TS} estimates of 70-84% type sharing (Figure S5D). Additionally, the WGS study identified varcode6 and varcode7 in Colombian isolates from 2014-2016 and in 2016, respectively, but varcode4 was not identified in any of their Colombian isolates (56).

We were also interested to better understand the origins of those varcodes that did not cluster with the “outbreak cluster” since historically they may have been imported and may represent other locally circulating parasites that were not a direct result of onward transmission after the outbreak. We found evidence of two putative importations of parasites from neighboring countries, varcode9 from Colombia (Case EC53, Table 1), based on both genetic and epidemiologic data, and varcode5 (Case EC40, Table 1) the origin of which was less clear. The epidemiological data for the putative

infection location was recorded as Peru (Case EC40, Table 1), however based on our data this *varcode* is more related to historical *P. falciparum* populations from French Guiana and Venezuela than Peru. The remaining Ecuadorian isolates with *varcodes* 2 and 8 did not cluster with any other South American isolate. The epidemiological data for the putative infection location for *varcode8* was recorded as Colombia (EC49 and EC50, Table 1), but these isolates did not cluster with Colombian isolates in our network analysis. Sharing of DBL α types in these *varcodes* with Colombian types was high (44% for *varcode2* and 67% for *varcode8*, Figure 5D), providing evidence that parasites with *varcode2* and *varcode8* may represent residual parasites historically imported from Colombia. This is consistent with WGS data for isolates with *varcode2*, demonstrating they are identical by descent (IBD>0.99) with Colombian isolates from the early 2000s (56), suggesting past rather than recent importation. It is worth noting that *varcode2* was identified in the hotspot of San Lorenzo, Esmeraldas confirming that this location may act as a reservoir of parasites with diverse *var* repertoires, as described above.

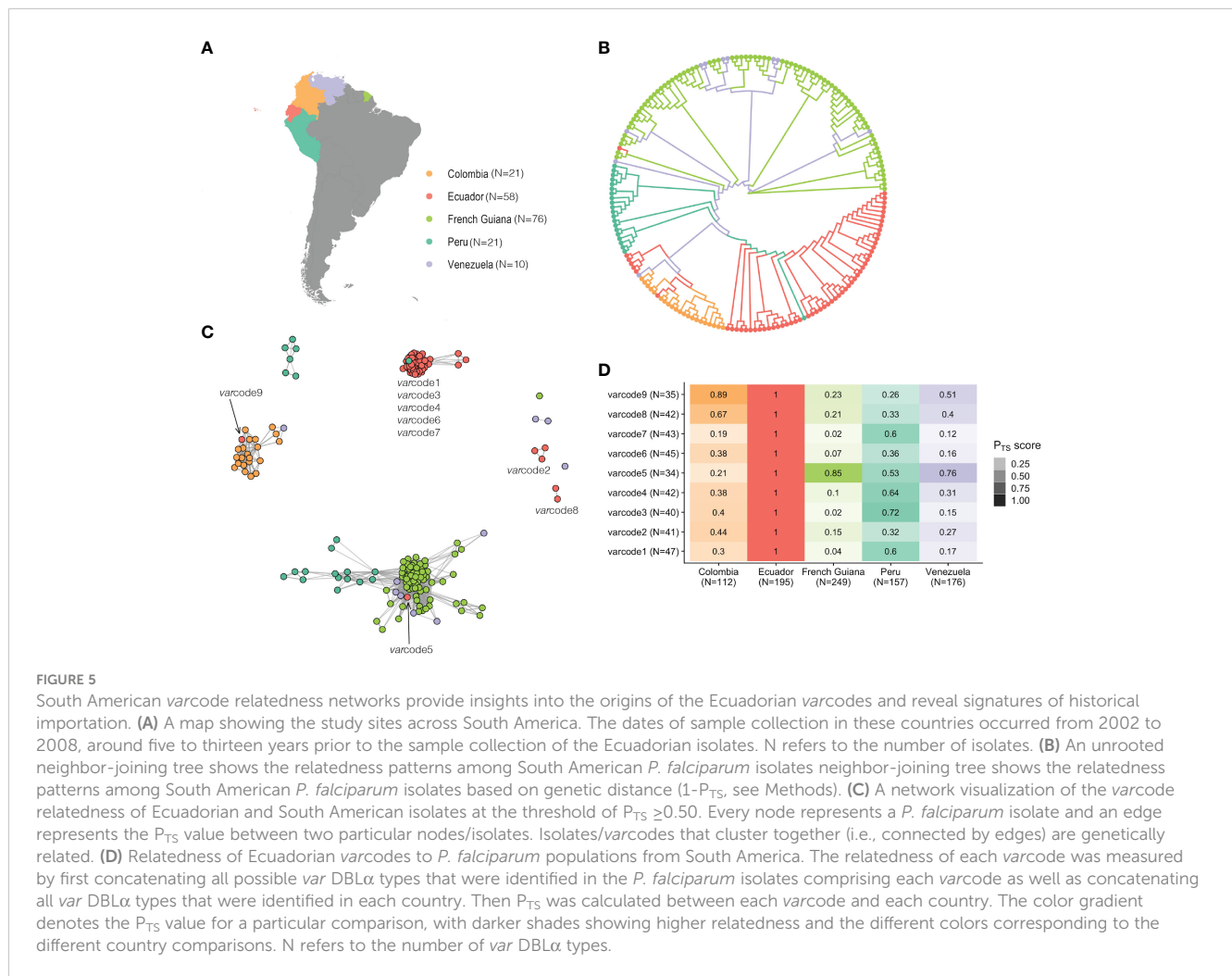
Discussion

Our investigation of the spatiotemporal incidence of clinical episodes of *P. falciparum* in Ecuador by *varcoding* supports the view that disease transmission after the 2012-2013 outbreak was sustained by parasites circulating in Ecuador, some of which may have had historical origins in neighboring countries. We observed persistence of the outbreak clonal lineage (identified with the same *varcodes*) and parasites with highly related *varcodes* predominantly associated with clinical disease after the outbreak. The observed *varcode* relatedness signatures may point to potential outcrossing of the outbreak lineage with other locally circulating parasites. Whether these recombinant *varcodes* resulted from sexual recombination events between parasites with outbreak *varcode1* and genetically distinct parasites that were already circulating at low levels and/or in asymptomatic reservoirs in Ecuador [e.g. (12)] or those that were previously imported, could not be ascertained from the current study population. Our results point to the need for resources to be focused locally in Ecuador to uncover the circulating reservoirs of infection. In this context, *var* genes will undoubtedly play a role in the persistence and virulence of these parasites. A role for human mobility must also be considered in the spread of *P. falciparum* in Ecuador, as parasites with the same *varcodes* were also observed across large distances (~150-300km) and two putative importations from Colombia and Peru were identified based on both epidemiological and *varcoding* data.

San Lorenzo was found to be a transmission hotspot likely due to mining activities and occupation-related travel in these areas, as well as its proximity to the Ecuador-Colombia border (4, 35, 59–61). These findings point to San Lorenzo for both genetic surveillance and targeted interventions. Importantly, our results provide strong evidence for ongoing local transmission in Ecuador and provide the first baseline characterization of *P. falciparum* antigenic diversity and parasite *varcodes* circulating in the Ecuadorian northwest coast and Amazon regions. This forms a

historical database that can be leveraged in future molecular epidemiology studies. It is worth noting that *varcode5* identified in Orellana province, an area of the Amazon region that neighbors Peru, had a very different genetic profile to the other Ecuadorian *varcodes* ($\geq 83\%$ unique types). It is more genetically related to historical parasites from French Guiana and Venezuela pointing to highly diverse *P. falciparum* populations that are likely circulating in the Ecuadorian Amazon region and Ecuador-Peru border. Several recent outbreaks have occurred in the same border areas of Ecuador [in 2016 (9), 2018 (10), 2019 (11) and 2020 (62)]. Our findings of highly related and possible recombinant parasites of the outbreak clone causing clinical disease shortly after the outbreak may provide an explanation for how sustained epidemics of disease continue to occur locally. The importation of parasites combined with local transmission can clearly increase the pool of antigenic variants as well as overall genome diversity, although periodic outbreaks of local parasites may also provide sufficient conditions for this to occur locally in the absence of parasite importation.

We demonstrated that 58% of clinical cases sampled in 2014 immediately after the outbreak in Ecuador were caused by parasites with highly related or possibly recombinant *varcodes*. The same trend was observed in 2015, although our sampling was limited relative to the number of reported cases for the months sampled. Is this a chance finding, or a consequence of selection, i.e., drug or immune selection? Previously published drug-resistance marker genotyping data reported that all *P. falciparum* isolates in our study had genotypes associated with chloroquine-resistance (i.e., *pfcr1* 76T) and the majority had genotypes associated with sensitivity to sulfadoxine-pyrimethamine (i.e., *pfdhps* and *pfdhfr*) (36). Mutations in *pfdhfr* were only present in parasites with *varcode2* and one of the highly related *varcodes* (*varcode6*) but not the other *varcodes*. Past antimalarial treatment for *P. falciparum* malaria in Ecuador included artesunate and sulfadoxine-pyrimethamine alone or in combination with primaquine until 2012 when a switch to artemether-lumefantrine +primaquine was introduced as the first-line treatment (63). Thus, it does not appear from our findings that drug selection is associated with the *var* population structure we observe in clinical cases after the outbreak. Therefore, we hypothesize that parasites with these highly related *varcodes* have new or antigenically novel combinations of *var* DBL α types and possibly alleles of single copy diverse antigen-encoding genes. This may provide an advantage in a population with variable levels of immune memory, as would be expected for these communities in Ecuador where seroprevalence of antibodies against *P. falciparum* has been reported to be as high as 22% (12). Supporting this view, prior network analyses and computational models combining evolution and epidemiology point to variant-specific immune selection defining *var* population structure even in low transmission, albeit to a much lesser extent than expected in high-transmission settings where selection acts strongly against recombinant or highly related repertoires due to cross-immunity (37, 64). The availability of *var* DBL α sequences provides the potential to test this hypothesis by serological methods that measure variant-specific immunity, as shown in serological studies in Papua New Guinea (65) and the Brazilian Amazon (66). In addition, characterization of antigenic



variant var DBL α sequences could be leveraged in future gene expression studies to understand parasite virulence. Indeed, future investigations into a potential fitness advantage of varcode1 and how it may enhance malaria transmission are warranted, in addition to exploring the origins of more recent outbreaks and whether they are the same or new varcodes.

A previous study that included some of the same *P. falciparum* isolates from Esmeraldas City and San Lorenzo in the northwest coast described three main genetic clusters based on microsatellite genotyping (35). In contrast, when considering the same isolates, varcoding resolved six varcodes circulating. Similar observations have been described in an earlier study in Venezuela where sympatric parasites identical at neutral microsatellite loci were shown to have very different var repertoires (67). This is not surprising as varcoding is expected to provide higher resolution than microsatellite genotyping as we are looking at more loci, which are under selection. Importantly, our varcode membership designations are consistent with genomic lineages as defined by identity-by-descent (IBD) analyses (IBD ≥ 0.99) and “super-clusters” (IBD ≥ 0.80) from a recent whole genome sequencing (WGS) study of *P. falciparum* isolates from the Pacific Coast of Ecuador and Colombia collected in the early 2000s and in 2013–2017 (including 30 of the same isolates in this study) (56). Although *P. falciparum* WGS data exclude var

data due to the difficulty of assembling highly diverse variant antigen genes, the WGS results are consistent with the population structure we infer from varcoding. To our knowledge this is the first direct comparison of parasite relatedness inference as determined by WGS IBD and varcoding P_{TS} (and BP_{TS}) where, given the low transmission in this setting, defining population structure by neutral markers and varcoding appears to converge. This provides compelling evidence of the utility of varcoding and downstream P_{TS} and BP_{TS} analytical approaches in such settings. Indeed, it is noteworthy that varcoding predicted the same genomic lineages and resolved parasite relatedness in line with WGS analyses, with the added advantage of simultaneously providing surveillance information about the major variant surface antigen-encoding genes. An interesting line of inquiry beyond the scope of this study will be to explore whether IBD-based approaches can be applied to varcoding data, particularly in elimination settings where the population may be highly inbred and most infections are monoclonal.

Amplicon sequencing is being promoted as a potential cost-effective approach for molecular surveillance to inform on transmission patterns, potential parasite importation and parasite relatedness for malaria elimination efforts. Varcoding is a targeted amplicon sequencing approach requiring a single PCR with degenerate primers to amplify 40–60 genes from the var

multigene family encoding the most immunogenic protein family of *P. falciparum*. Here we demonstrate its potential as a cost effective and high-resolution method to examine *P. falciparum* antigenic diversity, parasite relatedness and genome-wide diversity patterns for molecular surveillance in low-transmission settings where highly related parasites are circulating. This will prove particularly useful in the context of changing patterns of human mobility and gene flow in the Americas where there is high demand for such a molecular surveillance method. Given that malaria elimination is achieved locally, *varcoding* may be useful in areas where WGS may not be conducted routinely, or where infrastructure and local capacity may not exist. Even in areas where WGS is routinely conducted, *varcoding* has the potential for screening samples and identifying the need for downstream WGS to save on resources. The tool will also be useful in other epidemic or low-transmission settings targeting elimination across the globe. Undoubtedly, going the distance to elimination by 2025 must be supported by appropriate molecular surveillance to better understand and track disease transmission as well as uncover the existence of local reservoirs of antigenically diverse parasites.

Data availability statement

The datasets presented in this study can be found in online repositories. The cleaned DBLα sequences generated in this study have been submitted to DDBJ/ENA/GenBank (BioProject Number: PRJNA642683). The python scripts for DBLα sequence processing can be found on GitHub in the following open-source repositories: DBLαCleaner pipeline (<https://github.com/Unimelb-Day-Lab/DBLαCleaner>); clusterDBLα pipeline (<https://github.com/Unimelb-Day-Lab/clusterDBLα>); classifyDBLα pipeline (<https://github.com/Unimelb-Day-Lab/classifyDBLα>) with a tutorial detailing the data processing workflow at <https://github.com/Unimelb-Day-Lab/tutorialDBLα>. All other deidentified data and analysis code are available on the open-source GitHub repository at <https://github.com/shaziaruybal/varcode-ecuador>.

Ethics statement

The studies involving human participants were reviewed and approved by Pontificia Universidad Católica del Ecuador and University of Melbourne. The patients/participants provided their written informed consent to participate in this study.

Author contributions

SR-P and KPD conceived and designed the study. FES and CAV-A carried out field work to obtain *P. falciparum* isolates and epidemiological metadata. SR-P and KET developed the *varcoding* methodology. SR-P and SLD performed the molecular experiments and sequencing; SR-P, FES and CAV-A curated the clinical and epidemiological metadata. SR-P performed the formal data analysis and visualization. EKJ and DBL designed and conducted the

Bayesian statistical analysis. SR-P, FES, KET and KPD contributed to the interpretation of the data. KPD supervised the work. SR-P, FES, and KPD acquired funding. SR-P and KPD wrote the paper with contributions from all authors. All authors contributed to the article and approved the submitted version.

Funding

This research was financially supported by the Pontificia Universidad Católica del Ecuador (grant numbers: L13058, L13248, M13416, N13416, O13087[QINV0084] to FES), the Fogarty International Center at the National Institutes of Health [Program on the Ecology and Evolution of Infectious Diseases (EEID), Grant number: R01-TW009670 to KPD], and the National Institutes of Allergy and Infectious Diseases, National Institutes of Health (grant number: R01-AI084156 to KPD). SR-P was supported by a Melbourne International Engagement Award from the University of Melbourne and gratefully acknowledges the J.D. Smyth Travel Award from the Australian Society for Parasitology that enabled her to travel to Ecuador to establish this collaboration.

Acknowledgments

The authors would like to thank the patients who contributed samples and the field teams who were involved in sample collections. We thank the Ecuadorian Ministry of Health, especially Luis E Castro, Julio Valencia and Javier Gomez Obando. We appreciate the support of the Australian Genome Research Facility for Illumina sequencing of the samples.

Conflict of interest

The authors declare that the research was conducted in the absence of any commercial or financial relationships that could be construed as a potential conflict of interest.

Publisher's note

All claims expressed in this article are solely those of the authors and do not necessarily represent those of their affiliated organizations, or those of the publisher, the editors and the reviewers. Any product that may be evaluated in this article, or claim that may be made by its manufacturer, is not guaranteed or endorsed by the publisher.

Supplementary material

The Supplementary Material for this article can be found online at: <https://www.frontiersin.org/articles/10.3389/fitd.2023.1085862/full#supplementary-material>

References

- Organization WH. *Eliminating malaria*. Geneva: World Health Organization (2016). Available at: <https://www.who.int/malaria/publications/atoz/eliminating-malaria/en/>.
- Organization WH. *Zeroing in on malaria elimination: Final report of the e-2020 initiative*. Geneva: World Health Organization (2021). Available at: <https://apps.who.int/iris/bitstream/handle/10665/340881/9789240024359-eng.pdf>.
- Espinoza J. Malaria resurgence in the Americas: An underestimated threat. *Pathogens* (2019) 8:11. doi: 10.3390/pathogens8010011
- Jaramillo-Ochoa R, Sippy R, Farrell DF, Cueva-Aponte C, Beltrán-Ayala E, Gonzaga JL, et al. Effects of political instability in Venezuela on malaria resurgence at Ecuador–Peru border, 2018. *Emerg Infect Dis* (2019) 25:834–6. doi: 10.3201/eid2504.181355
- Ferreira MU, Castro MC. Malaria situation in Latin America and the Caribbean: Residual and resurgent transmission and challenges for control and elimination. *Methods Mol Biol Clifton N J* (2019) 2013:57–70. doi: 10.1007/978-1-4939-9550-9_4
- Organization WH. *World malaria report 2019*. Geneva: World Health Organization (2019).
- Organization WH. *The e-2020 initiative of 21 malaria-eliminating countries: 2019 progress report*. Geneva: World Health Organization (2019).
- MSP. *Gaceta epidemiológica semanal no. 52*. Quito: Ministerio de Salud Pública del Ecuador (2016).
- MSP. *Gaceta epidemiológica semanal no. 52*. Quito: Ministerio de Salud Pública del Ecuador (2017).
- MSP. *Gaceta epidemiológica semanal no. 52*. Quito: Ministerio de Salud Pública del Ecuador (2018).
- MSP. *Gaceta epidemiológica semanal no. 52*. Quito: Ministerio de Salud Pública del Ecuador (2019).
- Sáenz FE, Arévalo-Cortés A, Valenzuela G, Vallejo AF, Castellanos A, Poveda-Loayza AC, et al. Malaria epidemiology in low-endemicity areas of the northern coast of Ecuador: high prevalence of asymptomatic infections. *Malaria J* (2017) 16:300. doi: 10.1186/s12936-017-1947-0
- Griffing SM, Mixson-Hayden T, Sridaran S, Alam MT, McCollum AM, Cabezas C, et al. South American plasmodium falciparum after the malaria eradication era: Clonal population expansion and survival of the fittest hybrids. *PLoS One* (2011) 6:e23486. doi: 10.1371/journal.pone.0023486
- Larrañaga N, Mejía RE, Hormaza JJ, Montoya A, Soto A, Fontecha GA. Genetic structure of plasmodium falciparum populations across the Honduras-Nicaragua border. *Malaria J* (2013) 12:354. doi: 10.1186/1475-2875-12-354
- Obaldia N, Baro NK, Calzada JE, Santamaria AM, Daniels R, Wong W, et al. Clonal outbreak of plasmodium falciparum infection in eastern Panama. *J Infect Dis* (2014) 211:1087–96. doi: 10.1093/infdis/jiu575
- Okoth SA, Chenet SM, Arrospe N, Gutierrez S, Cabezas C, Matta JA, et al. Molecular investigation into a malaria outbreak in cusco, Peru: Plasmodium falciparum BV1 lineage is linked to a second outbreak in recent times. *Am J Trop Med Hyg* (2015) 94:128–31. doi: 10.4269/ajtmh.15-0442
- Baldeviano GC, Okoth SA, Arrospe N, Gonzalez RV, Sanchez JF, Macedo S, et al. Molecular epidemiology of plasmodium falciparum malaria outbreak, tumbes, Peru, 2010–2012. *Emerg Infect Dis* (2015) 21:797–803. doi: 10.3201/eid2105.141427
- Chenet SM, Taylor JE, Blair S, Zuluaga L, Escalante AA. Longitudinal analysis of plasmodium falciparum genetic variation in turbo, Colombia: implications for malaria control and elimination. *Malaria J* (2015) 14:363. doi: 10.1186/s12936-015-0887-9
- Sáenz FE, Morton LC, Okoth SA, Valenzuela G, Vera-Arias CA, Vélez-Álvarez E, et al. Clonal population expansion in an outbreak of plasmodium falciparum on the northwest coast of Ecuador. *Malaria J* (2015) 14:497. doi: 10.1186/s12936-015-1019-2
- Carter TE, Malloy H, Existe A, Memnon G, Victor YS, Okech BA, et al. Genetic diversity of plasmodium falciparum in Haiti: Insights from microsatellite markers. *PLoS One* (2015) 10:e0140416. doi: 10.1371/journal.pone.0140416
- Dalmat R, Naughton B, Kwan-Gett TS, Slyker J, Stuckey EM. Use cases for genetic epidemiology in malaria elimination. *Malaria J* (2019) 18:163. doi: 10.1186/s12936-019-2784-0
- Neafsey DE, Taylor AR, MacInnis BL. Advances and opportunities in malaria population genomics. *Nat Rev Genet* (2021) 22:502–17. doi: 10.1038/s41576-021-00349-5
- Grenfell BT, Pybus OG, Gog JR, Wood JLN, Daly JM, Mumford JA, et al. Unifying the epidemiological and evolutionary dynamics of pathogens. *Science* (2004) 303:327–32. doi: 10.1126/science.1090727
- Volz EM, Koelle K, Bedford T. Viral phylodynamics. *PLoS Comput Biol* (2013) 9:e1002947. doi: 10.1371/journal.pcbi.1002947
- Barton N. Understanding adaptation in large populations. *PLoS Genet* (2010) 6:e1000987. doi: 10.1371/journal.pgen.1000987
- Rask TS, Hansen DA, Theander TG, Pedersen AG, Lavstsen T. Plasmodium falciparum erythrocyte membrane protein 1 diversity in seven genomes – divide and conquer. *PLoS Comput Biol* (2010) 6:e1000933. doi: 10.1371/journal.pcbi.1000933
- Otto TD, Assefa SA, Böhme U, Sanders MJ, Kwiatkowski Consortium P, et al. Evolutionary analysis of the most polymorphic gene family in falciparum malaria. *Wellcome Open Res* (2019) 4:193. doi: 10.12688/wellcomeopenres.15590.1
- Barry AE, Leliwa-Sytek A, Tavul L, Imrie H, Migot-Nabias F, Brown SM, et al. Population genomics of the immune evasion (var) genes of plasmodium falciparum. *PLoS Pathog* (2007) 3:e34. doi: 10.1371/journal.ppat.0030034
- Chen DS, Barry AE, Leliwa-Sytek A, Smith T-A, Peterson I, Brown SM, et al. A molecular epidemiological study of var gene diversity to characterize the reservoir of plasmodium falciparum in humans in Africa. *PLoS One* (2011) 6:e16629. doi: 10.1371/journal.pone.0016629
- Rougeron V, Tiedje KE, Chen DS, Rask TS, Gamboa D, Maestre A, et al. Evolutionary structure of plasmodium falciparum major variant surface antigen genes in south America: Implications for epidemic transmission and surveillance. *Ecol Evol* (2017) 7:9376–90. doi: 10.1002/ece3.3425
- Tonkin-Hill G, Ruybal-Pesántez S, Tiedje KE, Rougeron V, Duffy MF, Zakeri S, et al. Evolutionary analyses of the major variant surface antigen-encoding genes reveal population structure of plasmodium falciparum within and between continents. *PLoS Genet* (2021) 17:e1009269. doi: 10.1371/journal.pgen.1009269
- Day KP, Artzy-Randrup Y, Tiedje KE, Rougeron V, Chen DS, Rask TS, et al. Evidence of strain structure in plasmodium falciparum var gene repertoires in children from Gabon, West Africa. *Proc Natl Acad Sci* (2017) 114:E4103–11. doi: 10.1073/pnas.1613018114
- Ruybal-Pesántez S, Tiedje KE, Tonkin-Hill G, Rask TS, Kanya MR, Greenhouse B, et al. Population genomics of virulence genes of plasmodium falciparum in clinical isolates from Uganda. *Sci Rep-uk* (2017) 7:11810. doi: 10.1038/s41598-017-11814-9
- Lucchi NW, Narayanan J, Karell MA, Xayavong M, Kariuki S, DaSilva AJ, et al. Molecular diagnosis of malaria by photo-induced electron transfer fluorescent primers: PET-PCR. *PLoS One* (2013) 8:e56677. doi: 10.1371/journal.pone.0056677
- Vera-Arias CA, Castro LE, Gómez-Obando J, Sáenz FE. Diverse origin of plasmodium falciparum in northwest Ecuador. *Malaria J* (2019) 18:251. doi: 10.1186/s12936-019-2891-y
- Valenzuela G, Castro LE, Valencia-Zamora J, Vera-Arias CA, Rohrbach P, Sáenz FE. Genotypes and phenotypes of resistance in Ecuadorian plasmodium falciparum. *Malaria J* (2019) 18:415. doi: 10.1186/s12936-019-3044-z
- He Q, Pilosof S, Tiedje KE, Ruybal-Pesántez S, Artzy-Randrup Y, Baskerville EB, et al. Networks of genetic similarity reveal non-neutral processes shape strain structure in plasmodium falciparum. *Nat Commun* (2018) 9:1817. doi: 10.1038/s41467-018-04219-3
- Taylor HM, Kyes SA, Harris D, Kriek N, Newbold CI. A study of var gene transcription *in vitro* using universal var gene primers. *Mol Biochem Parasit* (2000) 105:13–23. doi: 10.1016/s0166-6851(99)00159-0
- Roche. *Using multiplex identifier (MID) adaptors for the GS FLX titanium chemistry—extended MID set* (2009). Available at: <https://dna.uga.edu/wp-content/uploads/sites/51/2013/12/GS-FLX-Titanium-General-Library-Preparation-Method-Manual-Roche.pdf>.
- Ruybal-Pesántez S, Tiedje KE, Pilosof S, Tonkin-Hill G, He Q, Rask TS, et al. Age-specific patterns of DBL α var diversity can explain why residents of high malaria transmission areas remain susceptible to plasmodium falciparum blood stage infection throughout life. *Int J Parasitol* (2021) 52(11):721–31. doi: 10.1016/j.ijpara.2021.12.001
- Oksanen J, Blanchet FG, Friendly M, Kindt R, Legendre P, McGlenn D, et al. *Vegan: Community ecology package* (2019). Available at: <https://CRAN.R-project.org/package=vegan>.
- Larremore DB. Bayes-optimal estimation of overlap between populations of fixed size. *PLoS Comput Biol* (2019) 15:e1006898. doi: 10.1371/journal.pcbi.1006898
- Johnson EK, Larremore DB. Bayesian Estimation of community size and overlap from random subsamples. *PLoS Comput Biol* (2022) 18:e1010451. doi: 10.1371/journal.pcbi.1010451
- Otto TD, Böhme U, Sanders M, Reid A, Bruske EI, Duffy CW, et al. Long read assemblies of geographically dispersed plasmodium falciparum isolates reveal highly structured subtelomeres. *Wellcome Open Res* (2018) 3:52. doi: 10.12688/wellcomeopenres.14571.1
- Pedersen TL. *Ggraph: An implementation of grammar of graphics for graphs and networks* (2020). Available at: <https://CRAN.R-project.org/package=ggraph>.
- Pedersen TL. *Tidygraph: A tidy API for graph manipulation*. (2019). Available at: <https://CRAN.R-project.org/package=tidygraph>.
- Dunnington D. *Ggsatial: Spatial data framework for ggplot2* (2018). Available at: <https://CRAN.R-project.org/package=ggsatial>.
- Pedersen TL, Robinson D. *Gganimate: A grammar of animated graphics* (2020). Available at: <https://CRAN.R-project.org/package=gganimate>.
- Kolde R. *Pheatmap: Pretty heatmaps* (2019). Available at: <https://CRAN.R-project.org/package=pheatmap>.
- Paradis E, Schliep K. Ape 5.0: an environment for modern phylogenetics and evolutionary analyses in R. *Bioinformatics* (2018) 35:526–8. doi: 10.1093/bioinformatics/bty633

51. Yu G, Smith DK, Zhu H, Guan Y, Lam TT. ggtree: an R package for visualization and annotation of phylogenetic trees with their covariates and other associated data. *Methods Ecol Evol* (2016) 8:28–36. doi: 10.1111/2041-210x.12628
52. Yu G, Lam TT-Y, Zhu H, Guan Y. Two methods for mapping and visualizing associated data on phylogeny using ggtree. *Mol Biol Evol* (2018) 35:3041–3. doi: 10.1093/molbev/msy194
53. Team RC. R: A language and environment for statistical computing. Vienna, Austria: R Foundation for Statistical Computing (2019). Available at: <https://www.R-project.org/>.
54. Wickham H, François R, Henry L, Müller K. Dplyr: A grammar of data manipulation (2020). Available at: <https://CRAN.R-project.org/package=dplyr>.
55. Stevenson M. epiR: Tools for the analysis of epidemiological data (2020). Available at: <https://CRAN.R-project.org/package=epiR>.
56. Carrasquilla M, Early AM, Taylor AR, Ospina AK, Echeverry DF, Anderson TJ, et al. Resolving drug selection and migration in an inbred south American plasmodium falciparum population with identity-by-descent analysis. *PLoS Pathog* (2022) 18:e1010993. doi: 10.1371/journal.ppat.1010993
57. Branch OH, Sutton PL, Barnes C, Castro JC, Hussin J, Awadalla P, et al. Plasmodium falciparum genetic diversity maintained and amplified over 5 years of a low transmission endemic in the Peruvian Amazon. *Mol Biol Evol* (2010) 28:1973–86. doi: 10.1093/molbev/msq311
58. Echeverry DF, Nair S, Osorio L, Menon S, Murillo C, Anderson TJ. Long term persistence of clonal malaria parasite plasmodium falciparum lineages in the Colombian pacific region. *BMC Genet* (2013) 14:2. doi: 10.1186/1471-2156-14-2
59. Douine M, Mosnier E, Hingrat QL, Charpentier C, Corlin F, Hureau L, et al. Illegal gold miners in French Guiana: a neglected population with poor health. *BMC Public Health* (2017) 18:23. doi: 10.1186/s12889-017-4557-4
60. Douine M, Sanna A, Hiwat H, Briolant S, Nacher M, Belleoud D, et al. Investigation of a possible malaria epidemic in an illegal gold mine in French Guiana: an original approach in the remote Amazonian forest. *Malaria J* (2019) 18:91. doi: 10.1186/s12936-019-2721-2
61. Mosquera-Romero M, Zuluaga-Idárraga L, Tobón-Castaño A. Challenges for the diagnosis and treatment of malaria in low transmission settings in San Lorenzo, esmeraldas, Ecuador. *Malaria J* (2018) 17:440. doi: 10.1186/s12936-018-2591-z
62. MSP. Personal communication. Ministerio de Salud Pública (2020).
63. Aguilar-Velasco HM. *Malaria y espacio en el Ecuador del verde de paris a la eliminación de la enfermedad*. Quito, Ecuador: Universidad Andina Simón Bolívar, Sede Ecuador (2021). Available at: <http://hdl.handle.net/10644/8216>.
64. Pilosof S, He Q, Tiedje KE, Ruybal-Pesántez S, Day KP, Pascual M. Competition for hosts modulates vast antigenic diversity to generate persistent strain structure in plasmodium falciparum. *PLoS Biol* (2019) 17:e3000336. doi: 10.1371/journal.pbio.3000336
65. Barry AE, Trieu A, Fowkes FJI, Pablo J, Kalantari-Dehaghi M, Jasinskas A, et al. The stability and complexity of antibody responses to the major surface antigen of plasmodium falciparum are associated with age in a malaria endemic area. *Mol Cell Proteomics* (2011) 10:M111.008326. doi: 10.1074/mcp.m111.008326
66. Carlos BC, Fotoran WL, Menezes MJ, Cabral FJ, Bastos MF, Costa FTM, et al. Expressed var gene repertoire and variant surface antigen diversity in a shrinking plasmodium falciparum population. *Exp Parasitol* (2016) 170:90–9. doi: 10.1016/j.exppara.2016.09.006
67. Tami A, Ord R, Targett GA, Sutherland CJ. Sympatric plasmodium falciparum isolates from Venezuela have structured var gene repertoires. *Malaria J* (2003) 2:7. doi: 10.1186/1475-2875-2-7

COPYRIGHT

© 2023 Ruybal-Pesántez, Sáenz, Deed, Johnson, Larremore, Vera-Arias, Tiedje and Day. This is an open-access article distributed under the terms of the [Creative Commons Attribution License \(CC BY\)](https://creativecommons.org/licenses/by/4.0/). The use, distribution or reproduction in other forums is permitted, provided the original author(s) and the copyright owner(s) are credited and that the original publication in this journal is cited, in accordance with accepted academic practice. No use, distribution or reproduction is permitted which does not comply with these terms.